Polydisperse Model for the Hydrodynamics of Expanded-Bed Adsorption Systems

Bo Xue, Xiaodong Tong, and Yan Sun
Dept. of Biochemical Engineering, School of Chemical Engineering and Technology, Tianjin University, Tianjin 300072, P.R. China

A polydisperse model is established to describe the hydrodynamic behaviors of solid particles within an expanded-bed adsorption column. This model has been used to simulate bed expansions conducted by different researchers under various operating conditions, and good agreements are found between the experimental and simulated results. The model is effective in simulating not only the change of bed height with fluid velocity, but also the size distributions of solid particles at different axial positions. Due to nonuniform flow in the column and density distribution of the particles, the calculated bed voidage is somewhat different from the measured one for the bottom and top regions of the column.

Introduction

As a novel integrated purification technique, expanded-bed adsorption (EBA) is now widely used in downstream bioprocesses. This technique gained its popularity in academia and industry in the early 1990s, and has been extensively studied since then by Gailliot et al. (1990), Chase and Draeger (1992), Batt et al. (1995), Owen and Chase (1997), Feuser et al. (1998), Anspach et al. (1999), Clemmitt and Chase (2000), and Tong and Sun (2002a,b). The hydrodynamic characteristics of an EBA system has a significant effect on its adsorption performance, and, hence, plays an important role in the design, scale-up, control, and optimization of an EBA unit (Chang and Chase, 1996). To date, however, this issue has not been well understood, and recent studies on this subject are rare. Existing monodisperse models (Poncelet et al., 1990; Thelen and Ramirez, 1997, 1999), though capable of describing the change in bed height with the superficial velocity of the fluid, are oversimplified in that they treat the adsorbent particles used in EBA as single-sized ones. It had been experimentally confirmed by recent studies that the concentration and average particle diameter of solid adsorbents decline along the fluid-flow direction in the column (Willoughby et al., 2000; Bruce and Chase, 2001; Tong and Sun, 2002b). Due to their inherent properties, the monodisperse models fail to depict this crucial phenomenon of EBA operations.

With the development of liquid–solid two-phase flow theories and simulation techniques, it is now feasible to conduct particle-scale simulations in two- or three-dimensional (3-D) configurations (Schwarzer, 1995; Davis, 1996; Höfler and Schwarzer, 2000; Tory, 2000; Bürger et al., 2001). Although much progress has been made, more efforts are still needed for a better understanding of the screening mechanism of velocity fluctuations and hydrodynamic diffusions, which has been, and still is, one of the most attractive issues in this field (Davis, 1996; Brenner, 1999; Ackerson et al., 2001; Miguel and Pastor-Satorras, 2001; Kuusela and Ala-Nissila, 2001). On the other hand, some 1-D approaches are simple in form, but valuable even in applications where fully 3-D particle-scale approaches are possible (Bürger et al., 2001). Representative examples for this include the successful application of 1-D, polydisperse model to simulations of batch sedimentation (Bürger et al., 2001) and fluidized-bed classifiers (Chen et al., 2002a, b). Experiments on EBA show that, in contrast to its drastic change along the axial direction of the column, the particle-size distribution (PSD) of solid adsorbents is almost uniform along the radial direction (Willoughby et al., 2000; Bruce and Chase, 2001; Tong and Sun, 2002b). Considering these facts, we choose to build up a mathematical model for EBA in a 1-D configuration. Unlike the just-mentioned monodisperse models, our model takes into account the polydispersity of the particles. Mixtures containing N discrete species are employed to represent highly polydisperse particles with continuous size distributions. By comparing simulations with available experimental results of EBA, we demonstrate that our polydisperse model can well predict not only

Correspondence concerning this article should be addressed to Y. Sun.

macroscopic parameters such as bed height, but also PSD and local bed voidage at any axial position within an EBA column under various operating conditions.

Theory

We consider an EBA column with L the length and D the inner diameter containing a fluid and N species of spherical, equidensity solid particles. The particle species are numbered in descending order by their radii, so that $r_{p,1} > r_{p,2} > \ldots > r_{p,N}$. Since our model is an extension, from monodisperse to polydisperse suspensions, of the 1-D two-phase flow model proposed by Thelen and Ramirez (1999), we first recall some of their results.

Based on the continuity and linear momentum equations for the fluid and solid particles, Thelen and Ramirez (1999) derived the following force-balance equation (their Eq. 27, in our notations) for solid particles with small-particle Reynolds number

$$\phi(u_f - u_p) - D_{ax}\frac{\partial \phi}{\partial x} - \phi\frac{h(\phi)m_b g}{6\pi\eta r_p} = 0, \tag{1}$$

where m_b is the buoyant mass defined as (their Eq. 26)

$$m_b = \frac{4\pi r_p^3}{3}(\rho_p - \rho_f). \tag{2}$$

Assuming that Eq. 1 is also valid for polydisperse suspensions, we then get the following equations for each particle species in an EBA system

$$\phi_i(u_f - u_{p,i}) - D_{ax,i}\frac{\partial \phi_i}{\partial x} - \phi_i\frac{h_i m_{b,i} g}{6\pi\eta r_{p,i}} = 0, \quad i = 1, 2, \ldots, N \tag{3}$$

Here the hindered settling function (HSF) h_i depends on the local volumetric fractions of all the particle species, and so does the axial dispersion coefficient $D_{ax,i}$. Besides, they may still depend on other variables [for example, the HSF proposed by Patwardhan and Tien (1985) is also a function of particle diameter]. The subscript i for both the HSF and axial dispersion coefficient emphasizes that they may vary for different species. To comply with the widely used formula for multispecies particle systems (Masliyah, 1979; Patwardhan and Tien, 1985; Bürger et al., 2001), we define the buoyant mass as the mass difference between the solid particles and the suspension (Eq. 4), rather than that between the particles and the fluid (Eq. 2)

$$m_{b,i} = \frac{4\pi r_{p,i}^3}{3}(\rho_p - \rho_s) \tag{4}$$

The density of the suspension is the volumetric average of those of the fluid and solid particles, that is,

$$\rho_s = \epsilon\rho_f + \left(\sum_{i=1}^{N}\phi_i\right)\rho_p \tag{5}$$

The Stokes velocity of the ith species is formulated as

$$u_{ST,i} = \frac{4}{3}\frac{\pi r_{p,i}^3(\rho_p - \rho_f)g}{6\pi r_{p,i}\eta} = \frac{2r_{p,i}^2(\rho_p - \rho_f)g}{9\eta} \tag{6}$$

From Eqs. 3 to 6, we have, upon substitution and rearrangement,

$$\phi_i u_{p,i} = \phi_i u_f - D_{ax,i}\frac{\partial \phi_i}{\partial x} - \phi_i\left(1 - \sum_{i=1}^{N}\phi_i\right)h_i u_{ST,i} \tag{7}$$

The incompressibility of both the fluid and particles gives

$$\epsilon + \sum_{i=1}^{N}\phi_i = 1 \tag{8}$$

and

$$\epsilon u_f + \sum_{i=1}^{N}\phi_i u_{p,i} = u_a \tag{9}$$

Combining Eqs. 7 to 9 yields

$$u_f = \left(1 - \sum_{i=1}^{N}\phi_i\right)\sum_{i=1}^{N}\phi_i u_{ST,i}h_i + \sum_{i=1}^{N}D_{ax,i}\frac{\partial \phi_i}{\partial x} + u_a \tag{10}$$

Substituting Eq. 10 for Eq. 7, and then the expression for $\phi_i u_{p,i}$ into the continuity equations for the particles (Eq. 11), we finally get the governing equations of the EBA system (Eq. 12)

$$\frac{\partial \phi_i}{\partial t} + \frac{\partial}{\partial x}(\phi_i u_{p,i}) = 0, \quad i = 1, 2, \ldots, N \tag{11}$$

$$\frac{\partial \phi_i}{\partial t} + \frac{\partial}{\partial x} \times \left[\phi_i\left(1 - \sum_{i=1}^{N}\phi_i\right)\sum_{i=1}^{N}\phi_i u_{ST,i}h_i - \phi_i\left(1 - \sum_{i=1}^{N}\phi_i\right)h_i u_{ST,i} + \phi_i u_a\right] = \frac{\partial}{\partial x}\left(D_{ax,i}\frac{\partial \phi_i}{\partial x} - \phi_i\sum_{i=1}^{N}D_{ax,i}\frac{\partial \phi_i}{\partial x}\right), \quad i = 1, 2, \ldots, N \tag{12}$$

The initial and boundary conditions for the equation group are

$$u_{p,i} = u_{p,i,0} \quad \phi_i = \begin{cases} \phi_{i,0}, & 0 < x \le H_0 \\ 0, & H_0 < x < L \end{cases}, \quad \text{for } t = 0 \tag{12a}$$

$$\phi_i u_{p,i} = 0, \quad \text{for } x = 0,\ t > 0 \tag{12b}$$

$$\phi_i u_{p,i} = 0, \quad \text{for } x = L,\ t > 0 \tag{12c}$$

The HSF adopted in our model was the one proposed by Masliyah (1979). It states that all the local particle species, regardless of their sizes, are retarded to the same extent, and the hindrance effect is a function of the total solid concentration only

$$h_i = h = \left(1 - \sum_{i=1}^{N} \phi_i\right)^{n-2} \tag{13}$$

For the axial dispersion coefficient, we propose a new correlation with the applied fluidization velocity by a power law (Eq. 14). Consequently, this parameter, like the HSF, is independent of particle species too. The formulation of HSF and axial dispersion coefficient will be further discussed in later sections

$$\frac{1-\epsilon}{\epsilon}\frac{u_a \mu}{D_{ax,i}} = \frac{1-\epsilon}{\epsilon}\frac{u_a \mu}{D_{ax}} = \alpha\left(\frac{1-\epsilon}{\epsilon}\frac{\rho_f u_a \mu}{\eta}\right)^{\beta} \tag{14}$$

In the case where the wall effect of the EBA column is nonnegligible, the Stokes velocity of particles (Eq. 6) is multiplied by a correction factor, according to Khan and Richardson (1989)

$$u_{ST,i} = \frac{2r_{p,i}^2(\rho_p - \rho_f)g}{9\eta}\left[1 - 1.15\left(\frac{d_{p,i}}{D}\right)^{0.6}\right] \tag{6a}$$

Numerical Method

The governing equations (Eq. 12) have been solved numerically with one of the latest modern entropy-satisfying shock-capturing central difference schemes for nonlinear conservation laws and closely related convection-diffusion equations (Kurganov and Tadmor, 2000). This scheme features a small numerical viscosity (of the order $O(\Delta x)^{2r-1}$), and maintains its high-resolution independent of $O(1/\Delta t)$. Moreover, the authors proved that their second-order semidiscrete scheme satisfied the total-variation diminishing property for scalar problems (Kurganov and Tadmor, 2000). Recently, Bürger and coworkers applied this scheme to solutions of the kinematic sedimentation model for polydisperse suspensions, yielding satisfactory results (Bürger et al., 2001). In this work, we first turned the governing equations (Eq. 12) into ordinary differential equations (ODEs) by semidiscrete differencing (Kurganov and Tadmor, 2000), and then integrated the ODEs numerically with ODE23, a low-order ODE solver embedded in Matlab 5.3. The grid cells for the spatial discretization was set at 0.25 cm in all the calculations, and N, the number of particle species, was set at 35. Further decrease in the grid cell size or increase in N had little influence on the simulation results. Under these conditions, the running time of the program on a personal computer (Celeron 733 MHz, 64 M RAM) ranged from 2 h to 6 h for one batch. Solutions to the convection–diffusion equations (Eq. 12) have been compared with those equations without diffusion terms (that is, equations obtained by deleting the righthand side term of Eq. 12), and the results indicated that numerical diffusion was negligible with respect to the physical diffusion embedded in Eq. 12 (data not shown).

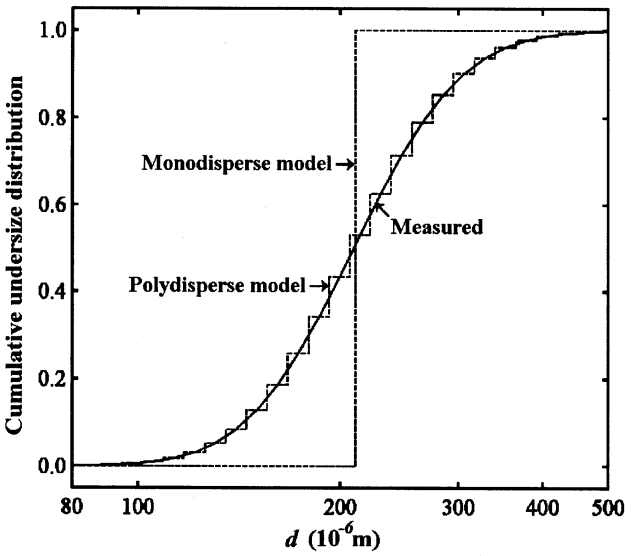

Figure 1. Comparison between particle sizes used in monodisperse and polydisperse models (N = 35).

Results and Discussion

Summary of model parameters

The polydisperse model proposed in this work has been used to simulate experiments conducted by several researchers under various operating conditions. Case I is on the dynamic response of bed height with step increase or decrease in fluidization velocity, which constitutes Thelen and Ramirez's previously published work (Thelen and Ramirez, 1999); Case II gives the variation of PSDs along the axial direction of the column with different settled bed heights, fluid viscosities, and fluidization velocities (Tong and Sun, 2002b). As part of Bruce and Chase's work, Case III reveals average particle concentrations within different bed zones (Bruce and Chase, 2001). Figure 1 clearly indicates how our polydisperse model differs from monodisperse models. All the parameters used in simulations are summarized in Table 1. The exponent n is obtained by fitting the Richardson-Zaki equation (Eq. 15) to corresponding experimental data on the relation between the fluidization velocity and average bed voidage (Thelen and Ramirez, 1999; Bruce and Chase, 2001; Tong and Sun, 2002b). As shown in Table 1, n is usually in the range from 4.3 to 5.0

$$u_a = u_t \cdot \epsilon^n \tag{15}$$

Theoretically, the settling velocities of polydisperse particles can be predicted by Stokes' law (Eq. 6a) with known physical properties of the fluid and the particles. Unfortunately, in many practical cases the prediction fails to match experimental observations (Thelen and Ramirez, 1999; Tong and Sun, 2002a), which may in part be attributed to experimental errors associated with the measurement of the parti-

cle and fluid properties. According to the analysis by Davis and Birdsell, the uncertainty in the predicted Stokes velocity is generally on the order of 5–10%, while careful measurements of the fall speed of the interface at the top of a settling suspension are accurate to within about 1% uncertainty (Davis and Birdsell, 1988). As a result, we chose to determine the average settling velocity of the polydisperse particles by data fitting. First, Eq. 6a is used to give an initial value of the settling velocity of the largest particle species ($i=1$), and the Stokes velocities for all the other $N-1$ particle species are calculated as follows

$$u_{ST,i} = u_{ST,1}\frac{r_{p,i}^2}{r_{p,1}^2}, \quad i = 2, 3, \ldots, N \tag{16}$$

The calculated velocities are then used to simulate bed expansion under certain operating conditions, and the simulated bed height is compared to the measured one. The $u_{ST,1}$ is adjusted according to the comparison, until the simulated and measured results match. The choice of the other two adjustable model parameters, α and β, though it plays an important role in determining the local PSD of the solid phase, has no significant impact on the simulated bed height. Therefore, the $u_{ST,i}$ determined by data fitting is unique and reliable.

Due to the porous nature of the STREAMLINE beads, the density difference between the hydrated beads and the fluid almost remains constant despite the change in the density of the fluid (because the beads are filled with the same fluid) (Xue and Sun, 2003). As a result, $u_{ST,1}$ (and also $u_{ST,i}$, $i=2, 3, \ldots, N$) varies roughly in inverse proportion to the viscosity of the fluid (Figure 2), which further justifies the $u_{ST,1}$ values listed in Table 1.

Table 1. Parameters Used in Simulations

Parameter	Case I*	Case II**	Case III†
Bead	STREAMLINE DEAE	STREAMLINE Base matrix	STREAMLINE SP
Type of PSD	Lognormal	Lognormal	Lognormal
μ (10^{-6} m)	211††	211	192
σ (10^{-6} m)	63††	63	51
H_0 (m)	0.157§	0.100 ~ 0.200	0.209
ϵ_0	0.40§	0.40	0.43
u_a (10^{-4} m/s)	1.27 ~ 4.67	1.97 ~ 10.28	5.28
n	4.3	5.0	5.0
$u_{ST,1}$ (10^{-2} m/s)	1.55	2.22, 1.12, 0.57	1.46
α	$1.02\cdot10^{-3}$	$1.02\cdot10^{-3}$	$8.87\cdot10^{-4}$
β	−0.5	−0.5	−0.5

*Conducted in 20% aqueous ethanol solution at 25°C ($\eta = 1.1\cdot10^{-3}$ Pa·s).
**Conducted at 20°C in distilled water ($\eta = 1.005\cdot10^{-3}$ Pa·s), 20 v/v% aqueous glycerol solution ($\eta = 2.025\cdot10^{-3}$ Pa·s), and 40 v/v% aqueous glycerol solution ($\eta = 4.878\cdot10^{-3}$ Pa·s). $u_{ST,1}$ values obtained with these fluids are 2.22, 1.12, $0.57\cdot10^{-2}$ m/s, respectively.
†Conducted in 50 mol/m^3 NaH_2PO_4 solution at room temperature.
††Only μ ($200\cdot10^{-6}$ m) was given by Thelen and Ramirez (1999), so the PSD of base matrix given in Case II was adopted as an approximation.
§Obtained by least-squares regression of experimental data (H vs. u_a) given by Thelen and Ramirez (1999).

Choice of HSF

Besides the Masliyah HSF (Eq. 13), there also exist many other HSFs in the literature, such as those proposed by Patwardhan and Tien (1985), Batchelor (1982), Davis and Gecol (1994), and Höfler and Schwarzer (2000). Recently, some researchers evaluated instability regions of polydisperse sedimentation equations with different HSFs (Biesheuvel et al., 2001; Bürger et al., 2002). Their chief findings were that for equidensity particles, the Masliyah HSF resulted in a system of first-order conservation laws that were always hyperbolic with arbitrary particle species and size distributions; substitution of the Masliyah HSF with other HSFs, for example, that by Davis and Gecol (1994), caused the model equations to change from hyperbolic to nonhyperbolic, or a mixed hyperbolic–elliptic type in certain regions. The occurrence of elliptic regions corresponded to some of the unstable modes that had been observed in sedimentation experiments (Batchelor and Rensburg, 1986). In this work, we confine the HSF in our model to the Masliyah HSF only to ensure that the problem is well posed.

Dispersion coefficient

As has been pointed out by Thelen and Ramirez (1999), the power law is a first attempt at correlating the solid-phase dispersion coefficient. Abundant examples of the implementation of this rule can be found in the literature (Dorgelo et al., 1985; Thelen and Ramirez, 1999; Chen et al., 2002a). In this article we propose a new correlation in a similar manner (Eq. 14). Under steady-state expansion, the mean velocity of any solid particles is zero, and from Eq. 9 we know

$$u_f = u_a/\epsilon, \tag{17}$$

and hence

$$u_f - u_a = \frac{1-\epsilon}{\epsilon}u_a \tag{18}$$

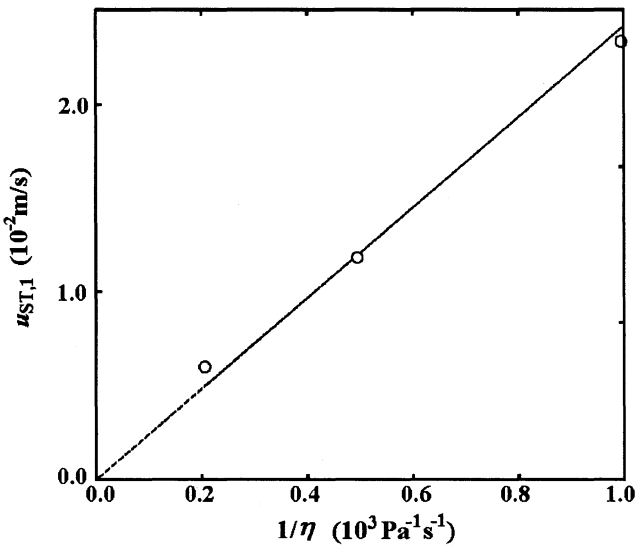

Figure 2. Influence of fluid viscosity on the settling velocity of solid particles.

The values of $u_{ST,1}$ and μ_f are given in Table 1. Solid line is the linear least-squares regression of the $u_{ST,1}$ data (circles) against μ_f^{-1}, indicating good proportionality between them.

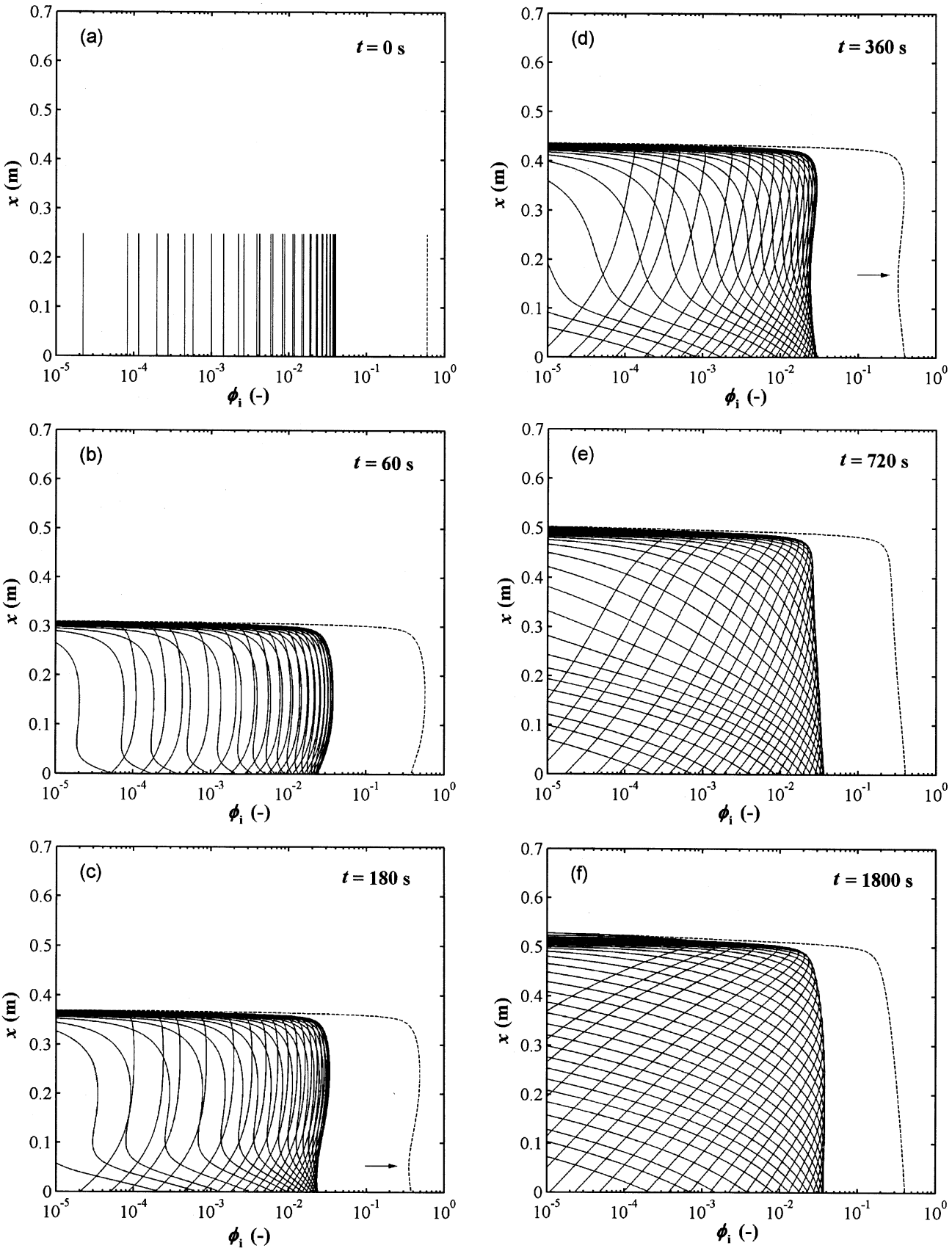

Figure 3. Simulated particle size and concentration distributions as a function of time and spatial distance.

Each solid line represents one particle species. Dashed line is the total volumetric fraction of the solid phase, whose local minimum is indicated by arrows in parts 3 (c) and (d).

It is thus clear that under steady state, the dispersion coefficient in Eq. 14 is correlated with the difference between the interstitial and apparent fluidization velocities. The positive dependence of D_{ax} on the interstitial fluidization velocity results in a decrease in D_{ax} from the lower part of the column, where the bed voidage is lower and the interstitial fluidization velocity is larger, to the upper part. As will be seen later, the PSD in an EBA column becomes narrower at higher positions, which implies the dispersion of solid particles is less severe in the upper part than in the lower part, so the decreasing trend of D_{ax} along the column seems consistent with experimental observations.

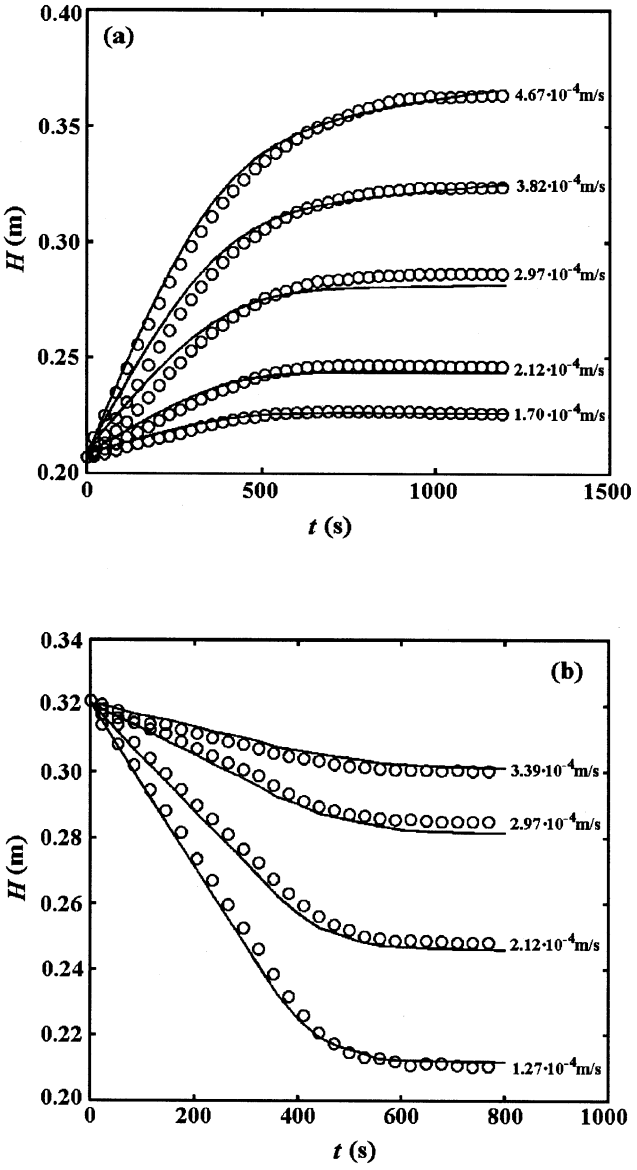

Figure 4. Dynamics of bed height with step changes in the fluidization velocity.

(a) Step increases from $1.27 \cdot 10^{-4}$ m/s to higher velocities, respectively, indicated in the figure. (b) Step decreases from $3.82 \cdot 10^{-4}$ m/s to lower velocities, respectively, indicated in the figure. Open circles were measurements by Thelen and Ramirez (1999). Solid lines are calculated from the polydisperse model. For more details, see Thelen and Ramirez (1999).

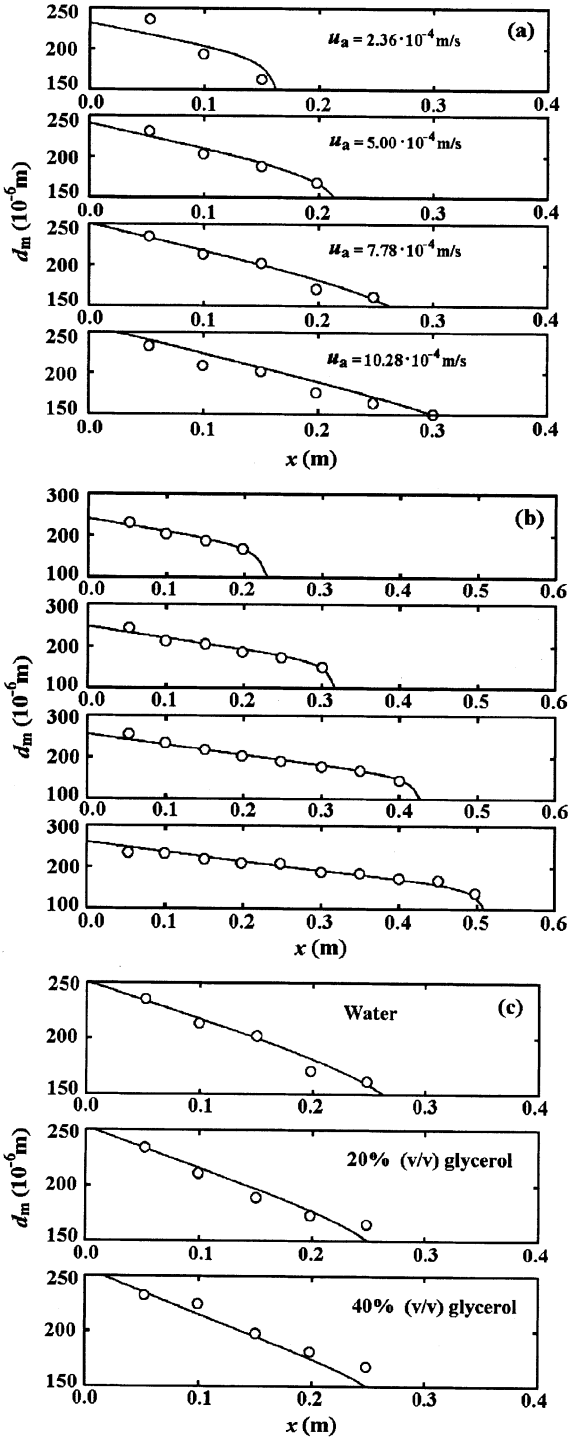

Figure 5. Local volume-weighted mean diameters of STREAMLINE beads at different heights within the EBA column (see also Table 1, Case II).

(a) Operations with different fluidization velocities. The fluid used in these operations was distilled water. The settled bed height was set at 0.10 m. (b) Operations with different initial (settled) bed heights. The bed was expanded to approximately two folds of its settled height. Applied fluidization velocities of the fluid (distilled water) were 5.00, 4.72, 5.00, and $4.72 \cdot 10^{-4}$ m/s, respectively (from top to bottom). (c) Operations with different fluid viscosities. The settled bed height was 0.10 m with a 2.5-fold bed expansion. Applied fluidization velocities of the fluid were 5.00, 3.78, and $1.97 \cdot 10^{-4}$ m/s, respectively (from top to bottom). Solid lines are calculated from the model.

Dynamic bed expansion

It is interesting to observe the dynamic procedure of bed expansion from one steady state (the settle bed in this work) to another. From Figure 3, we see clearly that at $t > 0$ disturbance caused by the upward flow of the fluid appeared at the bottom of the column; it traveled through the suspension, and finally disappeared at the interface between the clear liquid and the suspension. A local minimum of the total solid concentration was formed during this procedure, which is most obvious in Figures 3c and 3d (indicated by arrows). After about 30 min, a new steady state was achieved, and the profile of all the particle species remained unchanged afterwards (Figure 3f).

Change of bed height with fluid velocity

Figure 4 shows the dynamic response of bed height to a series of increases and decreases in fluid velocity (Case I). The agreement between the experimental and simulated results is as excellent as that obtained by Thelen and Ramirez (1999) with the monodisperse model, which demonstrates that the polydisperse model can be a good substitute for the monodisperse model in predicting bed-height dynamics.

PSDs at different column heights

Due to the difference in their settling velocities, the particle species are partly classified in the column. The beads near the bottom of the column are larger in mean diameter and have broader PSDs, while those near the top are smaller and distributed within narrower diameter ranges, which has been confirmed by the experimental results from Case II (Figures 5 and 6). The polydisperse model gives very good predictions of local mean particle diameters in the column (defined by Eq. 19) under various settled bed heights (Figure 5a), fluidization velocities (Figure 5b), and fluid viscosities (Figure 5c). The values of α and β are the same for all the conditions studied in Case II (Table 1), which suggests that Eq. 14 may act as a universal correlation for the dispersion coefficient of STREAMLINE beads. Figure 6, which corresponds to Figure 5b, shows the local PSD of STREAMLINE beads at different bed heights. At the major part of the column, the simulations match the experiments quite well. Small discrepancies that occur at the bottom and top of the column may be attributed to the turbulence and channeling in the zone right above the fluid distributor and the particle density distribution (PDD) of the STREAMLINE beads, which will be discussed further below. Another probable reason may be the underestimation of particle dispersion at the top region by Eq. 14, which can be inferred from the narrower profile of the predicted PSD curves when compared with the measured ones for this region. How to improve the accuracy in predicting D_{ax} is, therefore, an important issue that deserves further study

$$d_m = \sum_{i=1}^{N} \phi_i d_{p,i} / \sum_{i=1}^{N} \phi_i \qquad (19)$$

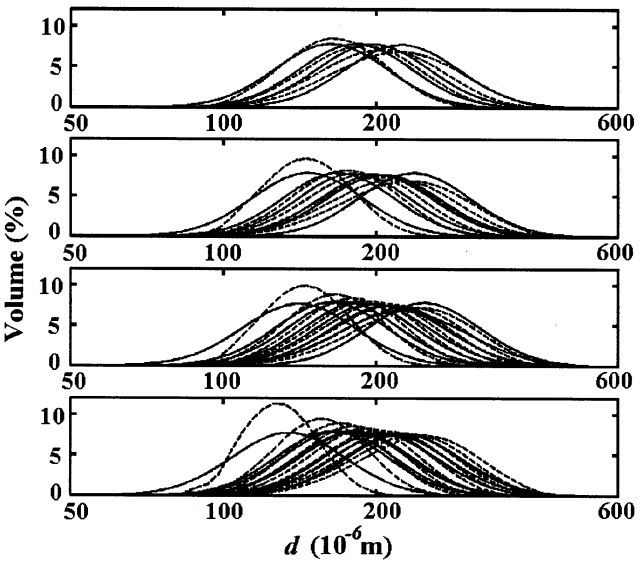

Figure 6. Particle-size distributions of the STREAMLINE beads at different heights within the EBA column.

For experimental details, see the legend to Figure 4b. Solid lines are experimental measurements. Dashed lines are calculated from the model.

Bed voidage

Although a bed's total voidage can be calculated readily from its initial (settled) height and voidage (usually 0.4), its local voidage at a given position is hard to determine. To date, only the average voidage of bed zones corresponding to at least one-fifth of the total bed volume has been reported, which was measured by the residence time distribution (RTD) method (Willoughby et al., 2000; Bruce and Chase, 2001). Table 2 gives the voidage measured by Bruce and Chase (Case III) along with that calculated from the polydisperse model. Again, the best match of experimental and theoretical results is located in the middle zone (0.10 ~ 0.25 m), which is in harmony with the conclusion drawn from the PSDs in Figure 6. The significant disagreements for the bottom and top zones are most likely caused by the following two reasons. The first is that the STREAMLINE beads are regarded as equidensity particles in the model. Although the density difference among STREAMLINE beads has been universally acknowledged, the actual PDD and its relation with PSD are still unknown at present because it is extremely difficult, if not impossible, to

Table 2. Measured and Calculated Bed Voidage in Different Column Zones

Bed Zone (m)	Average Bed Voidage		
	Measured*	Calculated	Error %
0 ~ 0.10	0.50	0.64	28.6
0.10 ~ 0.25	0.69	0.68	−1.2
0.25 ~ 0.40	0.86	0.76	−11.5
0 ~ 0.25	0.61	0.67	9.3
0 ~ 0.40	0.70	0.70	0.0

*Data from Bruce and Chase (2001).

determine them with available techniques. As a result, the PDD is not considered in the model. In a typical expanded bed, however, the average particle density varies from $1.19 \cdot 10^3$ kg/m^3 in the bottom quarter to $1.15 \cdot 10^3$ kg/m^3 in the top quarter of the column (Pharmacia, 1997). So, the actual voidage in the bottom and top zones was overestimated and underestimated, respectively, by the model that used the beads' average density lying between these two values. The second reason for the disagreements is the nonuniform flow in the zone between 0 and 0.10 m, which violates the assumption of laminar flow in deriving the model. Moreover, this phenomenon may shorten the residence time of tracers in this region, and, thus, make the estimated bed voidage by the RTD method smaller than the actual one (Bruce and Chase, 2001).

It is worth noting that the PDD should be treated with care, because in many cases its presence is the primary reason for the loss of hyperbolicity of equations modeling particle sedimentation (Biesheuvel et al., 2001; Bürger et al., 2002). The exclusion of it from our model, though making the model less accurate, ensures the admissibility of the central difference scheme used in this article. Measuring, as well as modeling, the PDD are both challenging problems to be solved in the future.

Conclusions

A polydisperse model is established to describe the hydrodynamics within an EBA column. This model has been tested against experimental results under various operating conditions. Agreements between the experimental and simulated results confirm its effectiveness in simulating not only the change of bed height with fluid velocity, but also the size distributions of solid particles at different axial positions. Due to nonuniform flow in the column and density distribution of the particles, the calculated bed voidage is somewhat different from the measured one for the bottom and top regions of the column. To further improve the accuracy of the model, more information on particle density distribution and nonuniform flow should be obtained and correctly accounted for in the model. The correlation for the dispersion coefficient, or the way to define particle dispersion in the model, is another issue that deserves in-depth investigation. Moreover, novel noninvasive methods are desired for accurate on-line measurements of local solid concentrations of each particle species. Some acoustic techniques (Alba et al., 1999; Stolojanu and Prakash, 2001) seem suitable for this purpose and might be employed in the future.

Acknowledgments

The financial support by the National Natural Science Foundation of China (Grant No. 20025617) is gratefully acknowledged. The authors also thank Dr. T. V. Thelen and Prof. W. F. Ramirez for allowing the use of their experimental data in this work.

Notation

d = particle diameter, m
D = inner diameter of the column, m
D_{ax} = axial dispersion coefficient of solid particles, m^2/s
h = hindered settling function
H = bed height, m
L = length of the column, m
m_b = buoyant mass, kg
n = exponent
N = number of particle species
r = particle radius, m
t = time, s
u = velocity, m/s
x = spatial variable (antiparallel to gravity), m

Greek letters

ϵ = volumetric fraction of the fluid
ϕ = volumetric fraction of the solid particles
η = fluid viscosity, Pa·s
μ = mean for particle diameter distribution, m
ρ = density, kg/m^3
σ = standard deviation for particle diameter distribution, m

Subscripts

0 = initial state
a = applied fluidization velocity
i = ith particle species
f = fluid
m = mean value
p = particle
ST = Stokes
s = suspension
t = terminal velocity in the Richardson-Zaki equation

Literature Cited

Ackerson, B. J., X. L. Lei, and P. Tong, "Subtle Order in Settling Suspensions," *Pure Appl. Chem.*, **73**, 1679 (2001).

Alba, F., G. M. Crawley, J. Fatkin, D. M. J. Higgs, and P. G. Kippax, "Acoustic Spectroscopy as a Technique for the Particle Sizing of High Concentration Colloids, Emulsions and Suspensions," *Coll. Surf. A: Physiochem. Eng. Aspects*, **153**, 495 (1999).

Anspach, F. B., D. Curbelo, R. Hartmann, G. Garke, and W.-D. Deckwer, "Expanded-Bed Chromatography in Primary Protein Purification," *J. Chromatogr. A*, **865**, 129 (1999).

Batchelor, G. K., "Sedimentation in a Dilute Polydisperse System of Interacting Spheres. Part 1. General Theory," *J. Fluid Mech.*, **119**, 379 (1982).

Batchelor, G. K., and R. W. J. V. Rensburg, "Structure Formation in Bidisperse Sedimentation," *J. Fluid Mech.*, **166**, 379 (1986).

Batt, B. C., V. M. Yabannavar, and V. Singh, "Expanded Bed Adsorption Process for Protein Recovery from Whole Mammalian Cell Culture Broth," *Bioseparation*, **5**, 41 (1995).

Biesheuvel, P. M., H. Verweij, and V. Breedveld, "Evaluation of Instability Criterion for Bidisperse Sedimentation," *AIChE J.*, **47**, 45 (2001).

Brenner, M. P., "Screening Mechanisms in Sedimentation," *Phys. Fluids*, **11**, 754 (1999).

Bruce, L. J., and H. A. Chase, "Hydrodynamics and Adsorption Behaviour Within an Expanded Bed Adsorption Column Studied Using In-Bed Sampling," *Chem. Eng. Sci.*, **56**, 3149 (2001).

Bürger, R., K.-K. Fjelde, K. Höfler, and K. Hvistendahl Karlsen, "Central Difference Solutions of the Kinematic Model of Settling of Polydisperse Suspensions and Three-Dimensional Particle-Scale Simulations," *J. Eng. Math.*, **41**, 167 (2001).

Bürger, R., K. H. Karlsen, E. M. Tory, and W. L. Wendland, "Model Equations and Instability Regions for the Sedimentation of Polydisperse Suspensions of Spheres," *Z. Angew. Math. Mech.*, **82**, 699 (2002).

Chang, Y. K., and H. A. Chase, "Development of Operating Conditions for Protein Purification Using Expanded Bed Techniques: The Effect of the Degree of Bed Expansion on Adsorption Performance," *Biotechnol. Bioeng.*, **49**, 512 (1996).

Chase, H. A., and N. M. Draeger, "Affinity Purification of Proteins Using Expanded Beds," *J. Chromatrogr.*, **597**, 129 (1992).

Chen, A., J. R. Grace, N. Epstein, and C. J. Lim, "Steady State Dispersion of Mono-Size, Binary and Multi-Size Particles in a Liquid Fluidized Bed Classifier," *Chem. Eng. Sci.*, **57**, 991 (2002a).

Chen, A., J. R. Grace, N. Epstein, and C. J. Lim, "Unsteady State Hydrodynamic Model and Dynamic Behaviour of a Liquid Fluidized Bed Classifier," *Chem. Eng. Sci.*, **57**, 1003 (2002b).
Clemmitt, R. H., and H. A. Chase, "Facilitated Downstream Processing of a Histidine-Tagged Protein from Unclarified *E. coli* Homogenates Using Immobilized Metal Affinity Expanded-Bed Adsorption," *Biotechnol. Bioeng.*, **67**, 206 (2000).
Davis, R. H., "Hydrodynamic Diffusion of Suspended Particles: A Symposium," *J. Fluid Mech.*, **310**, 325 (1996).
Davis, R. H., and K. H. Birdsell, "Hindered Settling of Semidilute Monodisperse and Polydisperse Suspensions," *AIChE J.*, **34**, 123 (1988).
Davis, R. H., and H. Gecol, "Hindered Settling Function with no Empirical Parameters for Polydisperse Suspensions," *AIChE J.*, **40**, 570 (1994).
Dorgelo, E. A. H., A. P. van der Meer, and J. A. Wesselingh, "Measurement of the Axial Dispersion of Particles in a Liquid Fluidized Bed Applying a Random Walk Method," *Chem. Eng. Sci.*, **40**, 2105 (1985).
Feuser, J., J. Walter, M. R. Kula, and J. Thommes, "Cell/Adsorbent Interactions in Expanded Bed Adsorption of Proteins," *Bioseparation*, **8**, 99 (1998).
Gailliot, F. P., C. Gleason, J. J. Wilson, and J. Zwarick, "Fluidized Bed Adsorption for Whole Broth Extraction," *Biotechnol. Progr.*, **6**, 370 (1990).
Höfler, K., and S. Schwarzer, "Navier-Stokes Simulation with Constraint Forces: Finite-Difference Method for Particle-Laden Flows and Complex Geometries," *Phys. Rev. E*, **61**, 7146 (2000).
Khan, A. R., and J. F. Richardson, "Fluid-Particle Interactions and Flow Characteristics of Fluidized Beds and Settling Suspensions of Spherical Particles," *Chem. Eng. Commun.*, **78**, 111 (1989).
Kurganov, A., and E. Tadmor, "New High-Resolution Central Schemes for Nonlinear Conservation Laws and Convection-Diffusion Equations," *J. Comp. Phys.*, **160**, 241 (2000).
Kuusela, E., and T. Ala-Nissila, "Velocity Correlations and Diffusion During Sedimentation," *Phys. Rev. E*, **63**(6), Article No. 061505 (2001).
Masliyah, J. H., "Hindered Settling in a Multi-Species Particle System," *Chem. Eng. Sci.*, **34**, 1166 (1979).
Miguel, M. C., and R. Pastor-Satorras, "Velocity Fluctuations and Hydrodynamic Diffusion in Sedimentation," *Europhys. Lett.*, **54**, 45 (2001).
Owen, R. O., and H. A. Chase, "Direct Purification of Lysozyme Using Continuous Counter-Current Expanded Bed Adsorption," *J. Chromatogr. A*, **757**, 41 (1997).
Patwardhan, V. S., and C. Tien, "Sedimentation and Liquid Fluidization of Solid Particles of Different Sizes and Densities," *Chem. Eng. Sci.*, **40**, 1051 (1985).
Pharmacia Biotech, *Expanded Bed Adsorption-Principles and Methods*, Uppsala, Sweden (1997).
Poncelet, D., H. Naveau, E.-D. Nyns, and D. Dochain, "Transient Response of a Solid-Liquid Model Biological Fluidized Bed to a Step Change in Fluid Superficial Velocity," *J. Chem. Technol. Biotechnol.*, **48**, 439 (1990).
Schwarzer, S., "Sedimentation and Flow Through Porous Media: Simulating Dynamically Coupled Discrete and Continuum Phases," *Phys. Rev. E*, **52**, 6461 (1995).
Stolojanu, V., and A. Prakash, "Characterization of Slurry Systems by Ultrasonic Techniques," *Chem. Eng. J.*, **84**, 215 (2001).
Thelen, T. V., and W. F. Ramirez, "Bed-Height Dynamics of Expanded Beds," *Chem. Eng. Sci.*, **52**, 3333 (1997).
Thelen, T. V., and W. F. Ramirez, "Modeling of Solid-Liquid Fluidization in the Stokes Flow Regime Using Two-Phase Flow Theory," *AIChE J.*, **45**, 708 (1999).
Tong, X.-D., and Y. Sun, "Nd-Fe-B Alloy-Densified Agarose Gel for Expanded Bed Adsorption of Proteins," *J. Chromatogr. A*, **943**, 63 (2002a).
Tong, X.-D., and Y. Sun, "Particle Size and Density Distributions of Two Dense Matrices in an Expanded Bed System," *J. Chromatogr. A*, **977**, 173 (2002b).
Tory, E. M., "Stochastic Sedimentation and Hydrodynamic Diffusion," *Chem. Eng. J.*, **80**, 81 (2000).
Willoughby, N. A., R. Hjorth, and N. J. Titchener-Hooker, "Experimental Measurement of Particle Size Distribution and Voidage in an Expanded Bed Adsorption System," *Biotechnol. Bioeng.*, **69**, 648 (2000).
Xue, B., and Y. Sun, "Modeling of Sedimentation of Polydisperse Spherical Beads with a Broad Size Distribution," *Chem. Eng. Sci.*, **58**, 1531 (2003).

Manuscript received Sept. 29, 2002, revision received Feb. 27, 2003, and final revision received Apr. 12, 2003.